Time Course of Metabolic Shifts in Cartilage Explants Exposed to Short-Term Simulated Microgravity

Eden Houske
Department of Biological and Environmental Sciences
Alyssa Hahn, PhD
May 1, 2023

Acknowledgements

First and foremost, I would like to thank my research advisor, Dr. Alyssa Hahn, for the opportunity to work in her lab. Her guidance has helped me grow confidence in a laboratory setting and has also aided me in developing an appreciation for research, especially pertaining to the field of orthopedics. My research experiences at Carroll College have taught me how to be resilient when the outcome of a procedure does not initially turn out as anticipated. I have learned to troubleshoot and optimize protocols by looking into relevant literature and this has ultimately led me to recognize the value in brainstorming and critical thinking. I am grateful to have reaped the rewards of successful research by presenting our scientific findings at multiple conferences. I would also like to thank my research partner, Matthew Glimm, for dedicating excessive amounts of time to carrying out this research and for being someone I can consult and exchange ideas with. Additionally, I would like to acknowledge the June Lab and the Montana State University Mass Spectrometry CORE Facility for their assistance with sample analysis. Finally, thank you to Dr. Brandon Sheafor and Dr. Ashley Beck for reviewing and critiquing this thesis and for being phenomenal and influential professors.

Abstract

Abnormal mechanical joint loading leads to an imbalance in chondrocyte metabolism that results in cartilage degeneration – a hallmark of osteoarthritis (OA). Microgravity exposure in space significantly reduces mechanical loads applied to the joints, leading to increased catabolic activity of chondrocytes and thus increasing the risk of OA. This study assesses how chondrocyte metabolism is altered in response to simulated microgravity (SM) exposure to gain insight into the mechanisms responsible for cartilage degeneration in reduced-loading environments. Healthy *post-mortem* human cartilage explants were exposed to SM for one or four days using a Rotating Wall Vessel (RWV) bioreactor and compared with the control explants exposed to normal gravitational forces. A subset of the control and SM explants were analyzed for cell viability by staining and measuring relative fluorescence. Metabolites were extracted from explants and surrounding media, and data were generated by liquid chromatography-mass spectrometry. Pathways upregulated in response to SM include the metabolism of pyrimidine, amino acids, and sugars, which may be suggestive of extracellular matrix remodeling. Changes in metabolites secreted from explants into the surrounding media mapped to lysine and vitamin E metabolism. These pathway changes have been previously detected in human synovial fluid from osteoarthritic donors, suggesting that even short-term SM exposure may induce metabolic shifts similar to that of early OA. Notably, this study is the first to map global metabolic changes in cartilage in response to short-term SM exposure to gain insight into the risk of developing OA post-spaceflight.

Table of Contents

Introduction

Articular cartilage is a specialized connective tissue that ensures lubrication and smooth movements in diarthrodial joints. It is composed of a dense network of fibers called the extracellular matrix (ECM) as well as chondrocytes which are distributed throughout. The ECM consists of collagen and proteoglycans which assist in joint lubrication by retaining water. Unlike other tissues of the musculoskeletal system, articular cartilage lacks blood vessels, nerves, and lymphatic vessels, thus limiting its healing capability in response to injury.[1] Instead, cartilage depends on receiving adequate nutrition by diffusion of molecules from the synovial fluid. Chondrocytes are limited in their ability to replicate due to the avascular nature of articular cartilage, so once they are damaged, the risk of joint injury can rise significantly.[1]

Damage that occurs to articular cartilage can lead to the development of a degenerative disease of the musculoskeletal system called osteoarthritis (OA).[2] In order for the joint to maintain proper homeostasis, cartilage and subchondral bone must be moderately loaded to reach a balance between anabolism and catabolism. Although articular cartilage is capable of withstanding high loads, the frequency and intensity of loading must be monitored in order to avoid degradation.[3] It is known that moderate mechanical loading of cartilage plays a role in healthy tissue remodeling as individuals who engage in regular physical activities have a decreased chance of developing OA.[4-8] In contrast, disruptions in normal loading conditions can cause chondrocytes to shift towards matrix catabolism, ultimately weakening the ability of articular cartilage to withstand large mechanical loads.[9] These shifts in normal loading conditions can be due to overloading, such as high impact forces,[10] or reduced loading, such as immobilization.[11] Both can lead to cartilage thinning and result in OA-like changes to the matrix. While the response of cartilage to overloading has been extensively studied,[10] more data are needed to elucidate the mechanisms underlying increased catabolism in cartilage as a result of exposure to reduced loading environments.

Multiple studies have preliminarily explored the effects of reduced loading on bone and cartilage.[12,13] In particular, bed rest studies are of interest because they can assess long-term changes in the musculoskeletal system as a result of a lack of joint loading.[14-16] Previous research has determined that bed rest in a 6° head-down tilt serves as a model to study the effects of reduced loading on the musculoskeletal system.[17] One study observed an 8% loss in average cartilage thickness superior to the tibia after 14 days of bed rest.[18] Another study observed a 2.9% reduction in cartilage at the patella and a 6.6% reduction at the medial tibia after seven weeks of partial weight bearing.[19] In addition to addressing cartilage thinning, reduced mechanical loading has been shown to have effects on chondrocyte signal transduction pathways.[20] These changes increase the catabolic activity of chondrocytes and cause structural damage to the ECM, including loss of proteoglycans and disturbances in collagen networks, which can eventually lead to the onset of OA.[21] Alterations in chondrocyte metabolism are not only concerning for individuals confined to their beds, but also those who are exposed to extended periods of unloading, such as astronauts. As space travel becomes increasingly frequent, there is still little known about the long-term effects of prolonged exposure to a microgravity environment on the musculoskeletal system.[22]

Previous studies have analyzed the effects of microgravity on cartilage through the use of *in vitro* models, *ex vivo* models, and by sending model organisms into space. *In vitro* models are beneficial because they typically are less costly, more feasible, allow for larger sample sizes, and provide easier control over confounding variables as opposed to the other experimental models.[23]

Chondrocytes cultured *in vitro* have exhibited a decrease in collagen and a rearrangement of the ECM within five days of exposure to microgravity.[24] However, the use of secondary cells may not accurately reflect the changes that occur within the primary chondrocytes of articular cartilage *in vivo*. Rather, the encapsulation of chondrocytes into a cylindrical agarose construct has been shown to provide a better model to simulate the consistency of articular cartilage.[25-29] A previous study performed by our lab investigated the metabolic effects of microgravity on chondrocytes that were encapsulated in cylindrical agarose constructs.[30] We found that short-term (< four days) exposure to microgravity did not induce large-scale shifts in chondrocyte metabolism. However, the metabolic shifts observed were consistent with early OA metabolomic profiles in human synovial fluid, suggesting that short-term exposure to microgravity could potentially lead to OA. Therefore, it is imperative that this field of research be more thoroughly investigated in order to promote the health of present and future astronauts.

Few studies have assessed the effects of simulated weightlessness on native bone and cartilage.[31] One study utilized spaceflight to unload rat joints and subsequently analyzed the effects on the rodents' bones.[32] Researchers identified a change in gene expression resulting in a reduced amount of calcified cartilage and bone, thus slowing the turnover of growth-plate cartilage and suppressing longitudinal bone growth. Another study exposed rodents to hind limb unloading and spaceflight for 30 and 13 days, respectively.[33] The rodents exhibited arthritic phenotypes that appeared to be remediated after recovery exercise. A third study exposed mice to microgravity for 30 days, and the articular cartilage post-spaceflight demonstrated a decrease in proteoglycan levels and downregulation of ECM molecules and genes.[34] Due to the downregulation of metabolites that typically protect against osteoarthritic changes, the researchers postulated that the articular cartilage was undergoing degradative changes. While these previous studies provide evidence of degenerative changes that occur in cartilage in response to microgravity and unloading, few, if any, studies have attempted to elucidate the underlying mechanism driving the degeneration.

The overall goal of this work was to assess how chondrocyte metabolism is altered in response to simulated microgravity (SM) exposure in order to gain insight into the mechanisms responsible for cartilage degeneration in reduced loading environments. This study offers a global view of metabolic changes that occur in primary chondrocytes in response to a lack of mechanical loading due to SM. This, in turn, allows for the comparison of perturbed metabolic pathways due to SM with altered pathways in osteoarthritic cartilage in order to gain insight into the risk of developing OA post-spaceflight. We achieve this aim through the exposure of *post-mortem* cartilage explants, showing no evidence of joint disease, to SM using a rotating wall vessel (RWV) bioreactor. Furthermore, the metabolites secreted into the surrounding media were analyzed as a model for early detection of OA in the synovial fluid. We showcase a novel method for studying chondrocyte mechanotransduction that more accurately reflects chondrocyte behavior *in vivo*.

Methods

Explant Acquisition and Culture

Human cartilage explants, purchased from Articular Engineering, were obtained from a post-mortem donor (male, age 84, Caucasian, cause of death: heart failure) with no evidence of joint disease and were cultured in Dulbecco's Modified Eagle's Medium (DMEM) supplemented

with 10% fetal bovine serum and 1% penicillin-streptomycin. Explants were incubated in 24 well plates in a 37ºC humidified atmosphere with 5% CO_2 prior to exposure to experimental or control conditions.

Experimental Design

Cartilage explants were weighed and randomly assigned to baseline (n=8), 1-day (n=16), or 4-day (n=24) time points. Half of the explants at each time point were inserted into individual cell culture vessels on a RWV bioreactor to maintain explants in free fall and to simulate microgravity (10^{-6} G) for a period of one or four days (1-day SM explants n=8; 4-day SM explants n=12).[35,36] The RWV bioreactor was positioned inside the incubator and was set at 13.6 rpm to maintain the explants in free fall for the duration of the SM exposure. Culture vessels were monitored throughout the experiment in order to ensure the explants were kept in free fall and to prevent bubble formation. The remaining explants were kept in cell culture vessels under standard culture conditions and normal gravitational forces for a period of one or four days to serve as controls (1-day control explants n=8; 4-day control explants n=12). Explants were sampled along with 1 mL aliquots of media from each culture vessel for metabolite extractions to profile changes in metabolism.

Cell Viability

A subset (n=4 per cohort) of the baseline and 1-day and 4-day control and SM explants were analyzed for cell viability. The explants were removed from culture vessels, subsequently washed with phosphate-buffered saline (PBS), and incubated in a solution containing 8 µmol calcein-AM and 75 µmol propidium iodide for 2 hours before analysis via Thermo Fisher Scientific Varioskan LUX multimode microplate reader. To detect relative fluorescence units (RFUs) for calcein-AM, the emission spectrum spanned from 508 - 600 nm with an excitation wavelength of 490 nm. For propidium iodide, the emission spectrum spanned from 555 - 650 nm with an excitation wavelength of 535 nm. The highest RFUs for each construct were obtained for calcein-AM and propidium iodide, and the mean values and standard deviations were calculated for each treatment group.

Metabolite Extraction

At the end of each time point, explants were removed from culture vessels and snap-frozen in liquid nitrogen. Explants were subsequently sliced into small pieces using a sterile scalpel. Cartilage was submerged in ice-cold 3:1 methanol:water solution and homogenized at 3000 rpm using a SPEX SamplePrep tissue homogenizer. Metabolites were extracted from both the surrounding media and homogenized explants using 80% v/v methanol, and samples were stored at -20ºC. Proteins were precipitated from the samples by adding 5 volumes of 1:1 aqueous acetonitrile solution and storing at 0ºC. Samples were vortexed and centrifuged throughout the extraction to remove cellular debris. Excess solvent was evaporated using a vacuum concentrator, and metabolite extracts were stored at -80ºC until mass spectrometry analysis.

Liquid Chromatography-Mass Spectrometry

Metabolites were resuspended in 50:50 water:acetonitrile solution for analysis by liquid chromatography-mass spectrometry (LC-MS) in positive mode. The LC-MS system used for data acquisition was an Agilent 1290 UPLC and Agilent 6538 Q-TOF mass spectrometer. Metabolites were separated on a Cogent Diamond Hydride HILIC 150 x 2.1 mm column using a normal phase gradient elution method.[37]

Statistical and Pathway Analyses

Data generated by the LC-MS were normalized to the median, log transformed, and standardized prior to analysis by univariate and multivariate statistical tests in MetaboAnalyst. The dataset was analyzed using hierarchical cluster analysis (HCA) visualized by clustergram for identification of clusters of co-regulated metabolites across time for pathway enrichment analyses. Metabolites from cartilage explants identified via fold change analysis were mapped to metabolic pathways to identify pathways that are upregulated or downregulated in response to microgravity. Unsupervised principal component analysis (PCA) and supervised partial least squares discriminant analysis (PLS-DA) were applied to visualize overall variation within the dataset. Metabolites with the highest variable importance in projection (VIP) scores from PLS-DA were mapped to metabolic pathways using the functional analysis feature in MetaboAnalyst. Significance for pathway analyses was determined with a false discovery rate (FDR) corrected p-value threshold < 0.05.

Results

Explant Viability

Viability of the cartilage explants was determined based on higher mean relative fluorescent units (RFUs) of calcein-AM relative to propidium iodide for the experimental and control cohorts at baseline, 1-day, and 4-day time points. Overall viability was estimated at > 90% across all time points and cohorts (**Figure 1**).

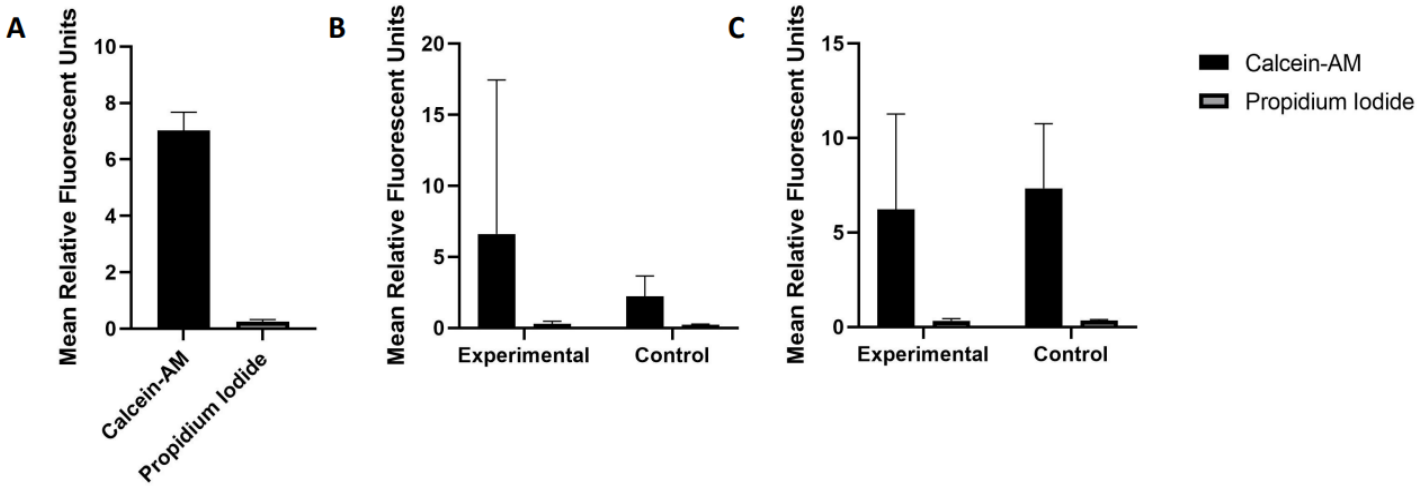

Figure 1. Cell viability of cartilage explants at **(A)** baseline, **(B)** 1-day, and **(C)** 4-day time points depicting mean relative fluorescent units and associated standard error bars. Calcein-AM stains viable cells while propidium iodide stains nonviable cells. (A) Mean RFUs for calcein-AM were 7.03 ± 0.46 and 0.24 ± 0.056 for propidium iodide. (B) Mean RFUs for calcein-AM in the experimental and control cohorts were 6.61 ± 5.42 and 2.23 ± 0.72, respectively. Mean RFUs for propidium iodide in the experimental and control cohorts were 0.29 ± 0.091 and 0.22 ± 0.025, respectively. (C) Mean RFUs for calcein-AM in the experimental and control cohorts were 6.23 ± 2.52 and 7.33 ± 1.71, respectively. Mean RFUs for propidium iodide in the experimental and control cohorts were 0.33 ± 0.055 and 0.34 ± 0.029, respectively.

Global Metabolomic Profiling of Explants and Media Exposed to Short-Term Simulated Microgravity

Global metabolomic profiling detected 9125 metabolite features across all samples. Unsupervised statistical analyses showcased overall variability within the dataset. PCA plots demonstrated that there was very little separation between the control and SM cohorts for both the cartilage explants and the surrounding media (**Figure 2**). Variability is depicted by how tightly each cohort is clustered, with more widespread clusters showcasing greater variability. For the explants, greater variability was identified within the 1-day control and 4-day SM cohorts (**Figure 2A**). For the media, greater variability was visualized within the 1-day and 4-day SM cohorts (**Figure 2B**).

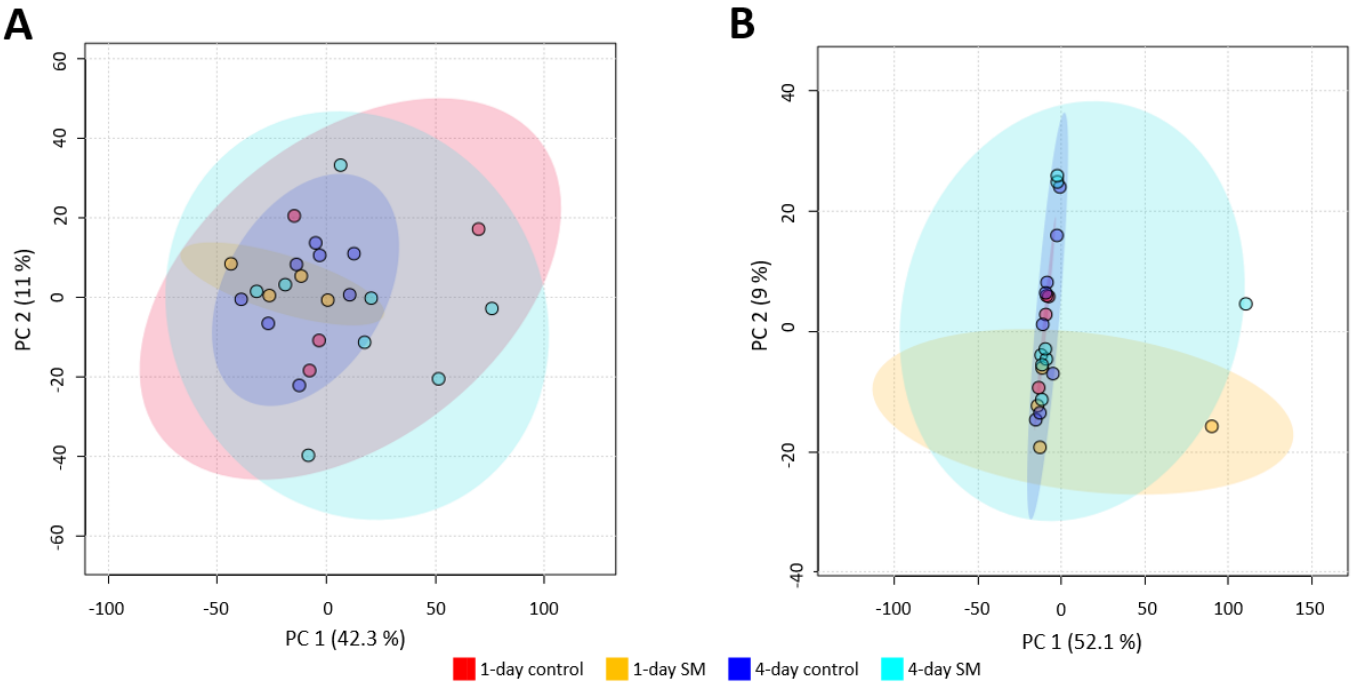

Figure 2. Unsupervised statistical plots depicting variation within and between cohorts for cartilage explants and media at both time points. Cohorts correspond to their respective color: red = 1-day control, orange = 1-day SM, dark blue = 4-day control, light blue = 4-day SM. **(A)** PCA plot showcasing minimal separation between the control and SM cartilage explants at 1-day and 4-day time points. The x-axis and y-axis principal components sum to 53.3% of the variation between cohorts. **(B)** PCA plot showcasing minimal separation between the control and SM media at 1-day and 4-day time points. The x-axis and y-axis principal components sum to 61.1% of the variation between cohorts.

Clustergram visualization demonstrated microgravity-induced changes in metabolism across time in cartilage explants and revealed clusters of co-regulated metabolites for pathway enrichment analysis (**Figure 3A**). Cluster 2 included metabolites that increased in concentration in response to both short-term SM time points, with these metabolites mapping to histidine, arginine, and proline metabolism, the urea cycle, and 3-oxo-10R-octadecatrienoate beta-oxidation (**Figure 3A**). Clusters 1 and 4 included metabolites that increased in concentration in at least one of the SM time points and mapped to histidine metabolism, pyrimidine metabolism, the urea cycle, glycerophospholipid metabolism, and butyrate metabolism (**Figure 3A**). Clusters 3 and 6 included metabolites that decreased in concentration in at least one of the SM time points with these metabolites mapping to lysine metabolism; valine, leucine, and isoleucine degradation; alkaloid biosynthesis; glycerophospholipid metabolism; vitamin E metabolism; coenzyme A catabolism; the urea cycle; fructose and mannose metabolism; and pyrimidine metabolism (**Figure 3A**). Clustergram visualization also highlighted microgravity-induced changes in metabolites secreted from cartilage explants across time and revealed clusters of co-regulated metabolites for pathway enrichment analysis (**Figure 3B**). Cluster 5 was the only cluster with co-regulated metabolites that mapped to significant pathways in pathway enrichment analysis. Cluster 5 included metabolites that increased in concentration in surrounding media at 4 days of SM exposure and mapped to lysine metabolism and vitamin E metabolism (**Figure 3B**). **Table 1** provides a comprehensive view of the pathways pertaining to each cluster.

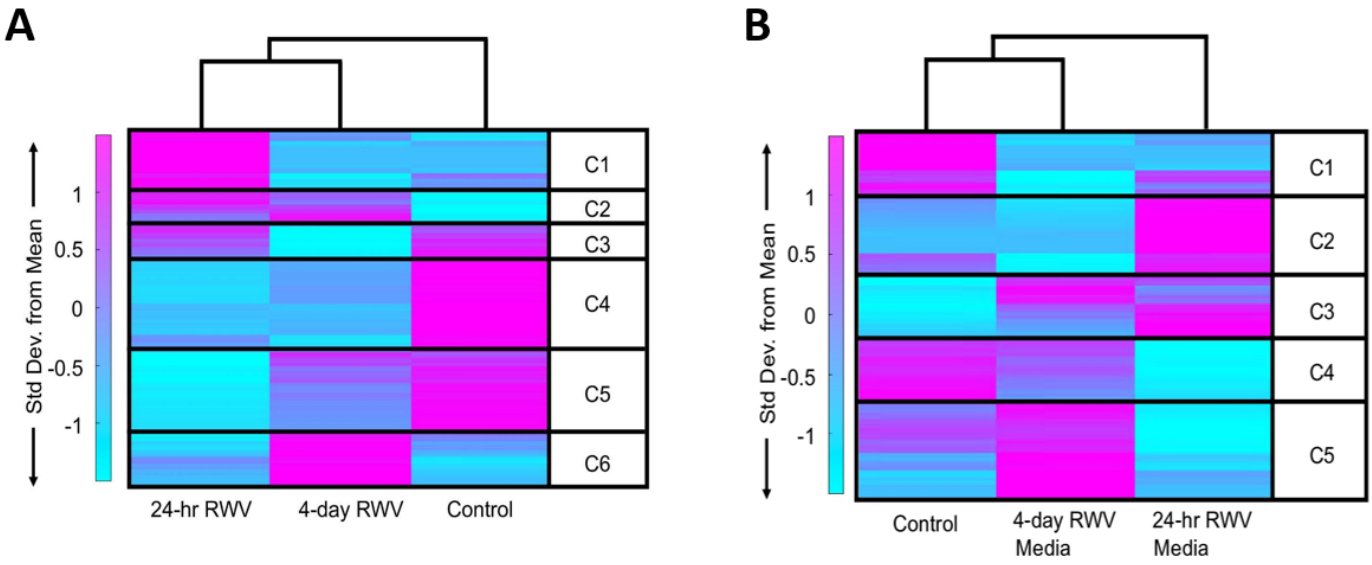

Figure 3. Unsupervised HCA and clustergram visualization depicting mean metabolite intensities in control and SM explants and surrounding media at 1-day and 4-day time points. Color is indicative of high (pink) or low (blue) mean metabolite intensity. Columns depict experimental and control cohorts across time while rows depict each individual metabolite's intensity based on standard deviation from the mean. **(A)** HCA clustergram showcasing changes in metabolism in cartilage explants at short-term SM time points (1-day SM, 4-day SM, and control comparison). **(B)** HCA clustergram showcasing changes in metabolites secreted from cartilage explants at short-term SM time points (control comparison, 4-day SM media, 1-day SM media).

Table 1. Pathway enrichment of HCA.

Cluster 2: ↑ 1-day and 4-day SM Explants	Clusters 1 & 4: ↑ SM Explants in at least one timepoint	Clusters 3 & 6: ↓ SM Explants in at least one timepoint	Cluster 5: ↑ 4-day SM Media
Amino acid metabolism (histidine, arginine, proline)	Histidine metabolism	Lysine metabolism	Lysine metabolism
The urea cycle	Pyrimidine metabolism	Amino acid degradation (valine, leucine, isoleucine)	Vitamin E metabolism
3-oxo-10R-octadecatrienoate beta-oxidation	The urea cycle	Alkaloid biosynthesis	
	Glycerophospholipid metabolism	Glycerophospholipid metabolism	
	Butyrate metabolism	Vitamin E metabolism	
		Coenzyme A catabolism	
		The urea cycle	
		Fructose and mannose metabolism	
		Pyrimidine metabolism	

Microgravity-Induced Metabolic Shifts in Articular Cartilage Explants

While HCA clustergram analysis helped visualize metabolic shifts across time and experiment groups, fold change analysis and PLS-DA with associated VIP scores were used to identify specific metabolic shifts at each time point in explants versus media. Fold change (FC) analysis involves a two-group comparison of the ratio of metabolite intensities. We identified seven significantly upregulated ($FC > 2$) and 16 significantly downregulated ($FC < 0.5$) pathways in 1-day SM explants compared to baseline explants. Upregulated pathways included

vitamin E metabolism; squalene and cholesterol biosynthesis; glycine, serine, alanine, and threonine metabolism; fatty acid metabolism; glycerophospholipid metabolism; and C21-steroid hormone biosynthesis and metabolism. Downregulated pathways included drug metabolism (cytochrome P450); tyrosine, lysine, tryptophan, and β-alanine metabolism; valine, leucine, isoleucine, and N-glycan degradation; vitamin B1, B3, and B6 metabolism; and linoleate, biopterin, butanoate, and glycerophospholipid metabolism. Fold change analysis comparing 4-day SM explants to baseline explants identified one significantly upregulated and 10 significantly downregulated pathways. Purine metabolism was upregulated, and downregulated pathways included putative anti-inflammatory metabolites; urea cycle/amino group metabolism; drug metabolism (cytochrome P450); valine, leucine, and isoleucine degradation; and methionine, cysteine, histidine, tryptophan, glycine, serine, threonine, linoleate, and vitamin E metabolism.

PLS-DA was used to visualize differences in the metabolic profiles between control and SM explants at 1-day and 4-day time points (**Figure 4**). PLS-DA allows for the detection of specific metabolites that contribute the most to the separation between cohorts. Clear separation between the control and SM cohorts was noted at the 1-day time point (**Figure 4A)**. Component 1 (53.3%) and Component 2 (12.7%) account for a total of 66% of the overall variability between the two cohorts. In contrast, there was some overlap observed between the control and SM cohorts at the 4-day time point (**Figure 4B**). Component 1 (41.3%) and Component 2 (8.5%) account for 49.8% of the variation between both cohorts. Metabolites with the highest VIP scores were mapped to metabolic pathways exhibited by **Tables 2 and 3** (FDR corrected p-value < 0.05). These pathways contribute the most to the separation between cohorts. Selected pathways for the 1-day time point include pyrimidine metabolism; valine, leucine, and isoleucine degradation; squalene and cholesterol biosynthesis; vitamin B1 metabolism; ascorbate and aldarate metabolism; and tryptophan metabolism. Pathways implicated in the 4-day time point include valine, leucine, and isoleucine degradation; amino acid metabolism; N-glycan biosynthesis; pyrimidine metabolism; coenzyme A biosynthesis; vitamin metabolism; glycerophospholipid metabolism; glycosphingolipid biosynthesis; starch and sucrose metabolism; and urea cycle/amino group metabolism. These results demonstrate that microgravity-induced metabolic shifts are detectable in articular cartilage even with short-term exposure.

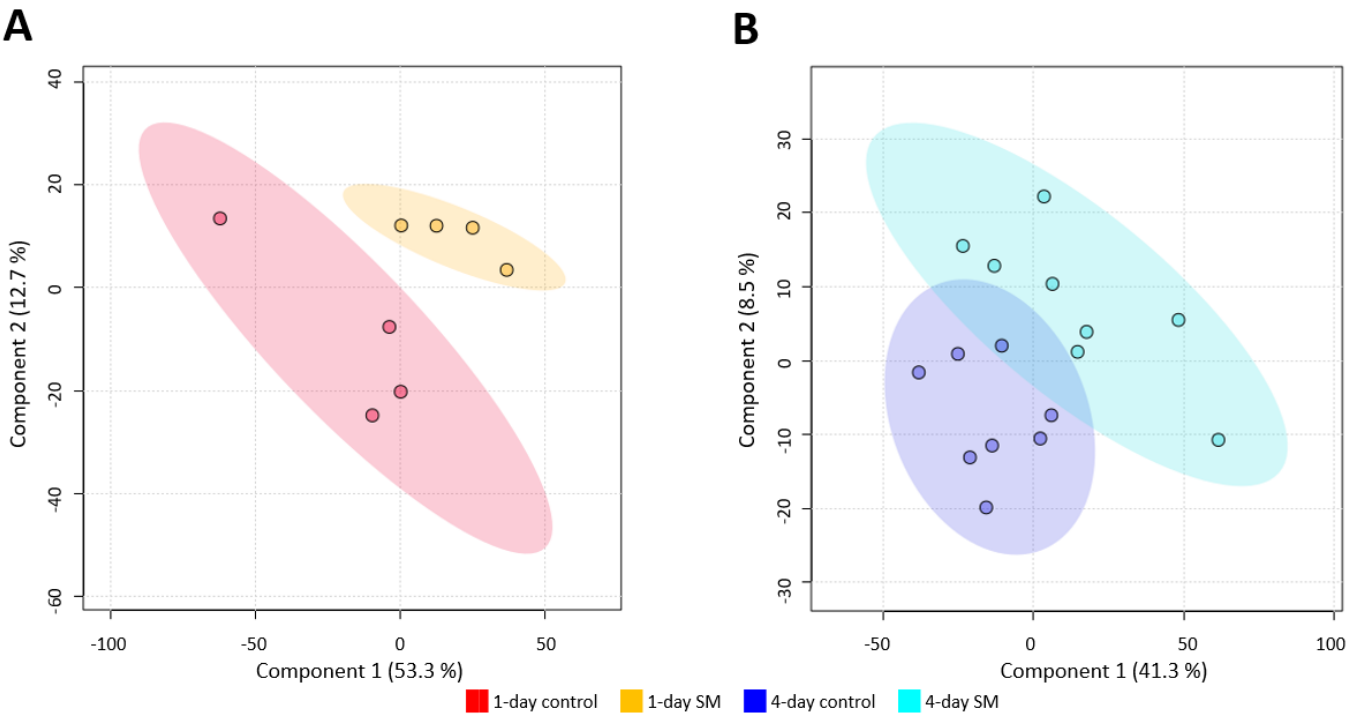

Figure 4. PLS-DA plots showcase differences in the metabolic profiles between control and SM explants at 1-day and 4-day time points. **(A)** PLS-DA plot demonstrating separation between control and SM cartilage explants at the 1-day time point. Components 1 and 2 sum to 66% of the overall variation between cohorts. Cohorts correspond to their respective color: red = 1-day control, orange = 1-day SM. **(B)** PLS-DA plot demonstrating some overlap between control and SM cartilage explants at the 4-day time point. Components 1 and 2 sum to 49.8% of the overall variation between cohorts. Cohorts correspond to their respective color: dark blue = 4-day control, light blue = 4-day SM.

Table 2. Pathway enrichment analysis of PLS-DA VIP scores for cartilage explants at 1-day time point.

Pathways	Metabolites Detected	FDR p-value
Pyrimidine metabolism	8	0.021
Valine, leucine, and isoleucine degradation	4	0.022
Squalene and cholesterol biosynthesis	3	0.022
Vitamin B1 (thiamin) metabolism	3	0.022
Ascorbate (Vitamin C) and aldarate metabolism	3	0.022
Drug metabolism – cytochrome P450	7	0.031
Tryptophan metabolism	14	0.043

Table 3. Pathway enrichment analysis of PLS-DA VIP scores for cartilage explants at 4-day time point.

Pathways	Metabolites Detected	FDR p-value
Valine, leucine, and isoleucine degradation	5	0.0086
Histidine metabolism	7	0.0091
Glycine, serine, alanine, and threonine metabolism	10	0.0092
N-Glycan biosynthesis	4	0.011
Alanine and aspartate metabolism	5	0.012
Pyrimidine metabolism	8	0.014
Vitamin B5 – CoA biosynthesis from pantothenate	4	0.018
Vitamin B1 (thiamin) metabolism	3	0.019
Ascorbate (Vitamin C) and aldarate metabolism	3	0.019
Drug metabolism – other enzymes	3	0.019
Glycerophospholipid metabolism	9	0.023
Methionine and cysteine metabolism	5	0.024
Arginine and proline metabolism	7	0.027
Lysine metabolism	8	0.033
Glycosphingolipid biosynthesis - ganglioseries	3	0.034
Starch and sucrose metabolism	4	0.043
Urea cycle/amino group metabolism	10	0.044

Microgravity-Induced Metabolic Shifts Detected in Surrounding Media

PLS-DA demonstrates that there are differences in the metabolic profiles between control and SM media at 1-day and 4-day time points (**Figure 5**). The control and SM media cohorts are largely separated and contain minimal overlap at the 1-day time point (**Figure 5A)**. Component 1 (54.6%) and Component 2 (20.9%) account for a total of 75.5% of the overall variability between the two cohorts. Likewise, there was also a small amount of overlap observed between the control and SM media at the 4-day time point (**Figure 5B**). Component 1 (48.3%) and Component 2 (11.7%) account for 60% of the variation between both cohorts. Metabolites with the highest VIP scores were mapped to metabolic pathways exhibited by **Tables 4 and 5** (FDR corrected p-value < 0.05). These pathways contribute the most to the separation between cohorts. Selected pathways for the 1-day time point include urea cycle/amino group metabolism; coenzyme A biosynthesis; valine, leucine and isoleucine degradation; and amino acid metabolism. Pathways implicated in the 4-day time point involved amino acid metabolism; squalene and cholesterol biosynthesis; butanoate metabolism; β-alanine metabolism; valine, leucine, and isoleucine degradation; vitamin B3 metabolism; and the carnitine shuttle. These

results demonstrate that microgravity-induced metabolic shifts are detectable in surrounding media even during short-term exposure.

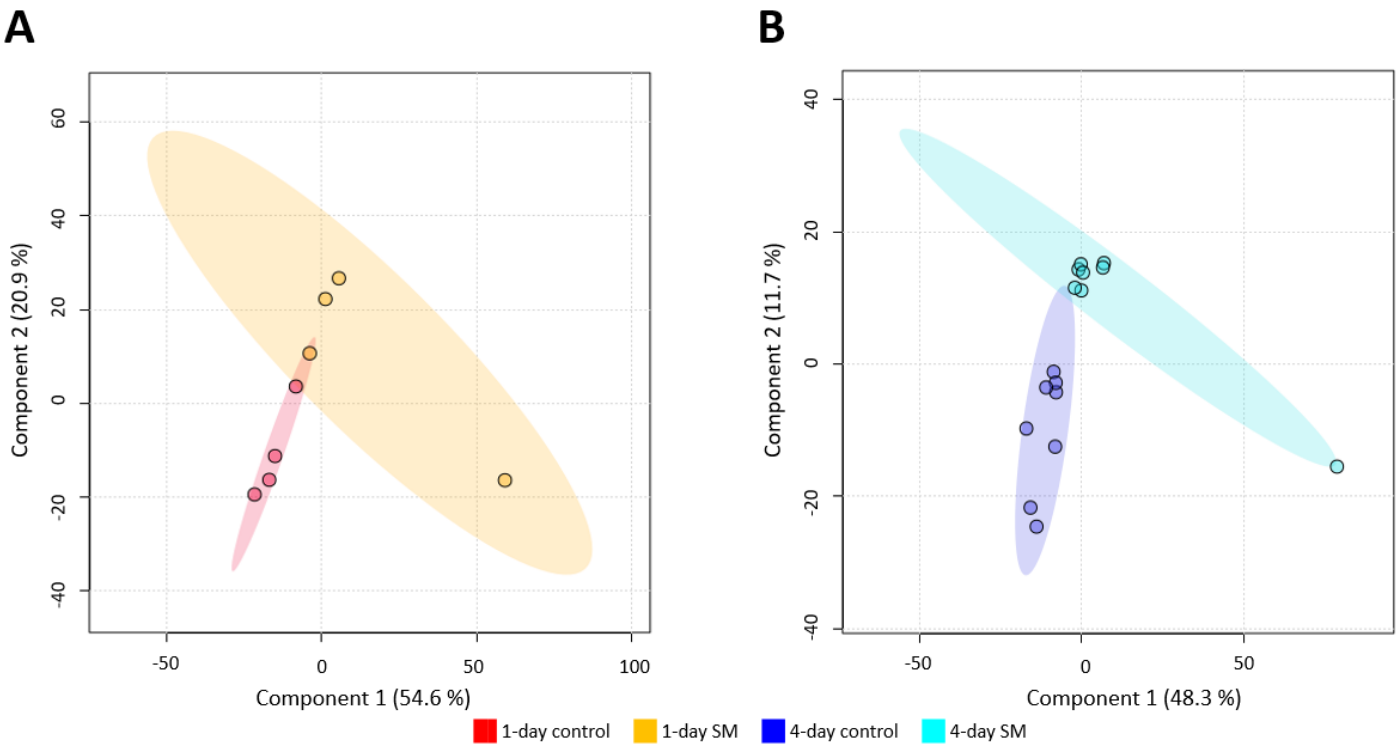

Figure 5. PLS-DA plots showcase differences in the metabolic profiles between control and SM secreted metabolites at 1-day and 4-day time points. **(A)** PLS-DA plot demonstrating minimal overlap between control and SM media at the 1-day time point. Components 1 and 2 sum to 75.5% of the overall variation between cohorts. Cohorts correspond to their respective color: red = 1-day control, orange = 1-day SM. **(B)** PLS-DA plot demonstrating separation between control and SM media at the 4-day time point. Components 1 and 2 sum to 60% of the overall variation between cohorts. Cohorts correspond to their respective color: dark blue = 4-day control, light blue = 4-day SM.

Table 4. Pathway enrichment analysis of PLS-DA VIP scores for surrounding media at 1-day time point.

Pathways	Metabolites Detected	FDR p-value
Urea cycle/amino group metabolism	17	0.021
Vitamin B5 – CoA biosynthesis from pantothenate	5	0.026
Valine, leucine, and isoleucine degradation	5	0.026
Lysine metabolism	13	0.029
Alanine and aspartate metabolism	6	0.038

Table 5. Pathway enrichment analysis of PLS-DA VIP scores for surrounding media at 4-day time point.

Pathways	Metabolites Detected	FDR p-value
Histidine metabolism	9	0.0083
Alanine and aspartate metabolism	6	0.012
Squalene and cholesterol biosynthesis	3	0.027
Butanoate metabolism	3	0.027
Ascorbate (Vitamin C) and aldarate metabolism	3	0.027
Glutamate metabolism	3	0.027
Beta-Alanine metabolism	3	0.027
Valine, leucine, and isoleucine degradation	4	0.027
Vitamin B3 (nicotinate and nicotinamide) metabolism	6	0.028
Arginine and proline metabolism	8	0.041
Pyrimidine metabolism	8	0.041
Carnitine shuttle	6	0.044

Discussion

Overview

To our knowledge, this study is the first to expose live healthy cartilage explants to SM using an RWV bioreactor to gain insight into metabolic shifts that occur in response to short-term SM exposure. Furthermore, this work significantly enhances our ability to study chondrocyte mechanotransduction in reduced mechanical loading environments in a manner that more accurately reflects chondrocyte behavior *in vivo*. We compared the results herein to our previous study exposing agarose-encapsulated chondrocytes to SM and found similarly perturbed metabolic pathways in cartilage in response to short-term SM, further validating our *in vitro* model.

Overall, we detected a total of 9125 metabolite features in cartilage explants and their surrounding media across 1-day and 4-day SM time points. The 4-day time point exhibited a greater number of significantly perturbed pathways compared to the 1-day time point in the cartilage explants (**Tables 2 and 3**) as well as in the media samples (**Tables 4 and 5**). This suggests that longer exposure to SM can potentially increase intracellular metabolic changes that occur in chondrocytes as a result of reduced joint loading.

Alterations in Chondrocyte Metabolism in Response to Microgravity

Notable metabolic pathways altered in cartilage in response to short-term SM included pyrimidine metabolism, amino acid metabolism, and sugar metabolism, all of which may be representative of ECM remodeling.[38-40] Restructuring the dense network of collagen and proteoglycans that comprise the ECM may place a higher energy demand on the chondrocytes. Furthermore, the detected alteration of N-glycan biosynthesis is suggestive of jeopardized lubrication. N-glycans are essential components of lubricin, a surface mucinous glycoprotein that

maintains cartilage integrity by providing lubrication and preventing the adhesion of cells and proteins.[41] Deleterious changes in the synthetic process of N-glycan could be indicative of osteoarthritic-like changes occurring in articular cartilage. Also of note were the perturbations observed in the urea cycle, amino group metabolism, purine metabolism, coenzyme A biosynthesis, and butyrate metabolism. Products pertaining to each of these pathways can be utilized by the TCA cycle to generate additional ATP when demand is elevated.[38] The identification of SM-induced alterations in these pathways is consistent with previous work that suggests chondrocytes exhibit ECM remodeling and fluctuating energy demands in response to SM.[30]

Vitamin metabolism was significantly perturbed in both cartilage and the surrounding media as a result of SM at both time points. Vitamins serve as cofactors for enzymes involved in the preservation of articular cartilage structure and function. Vitamins B5, C, and E serve as antioxidants and have been shown to impede the increased oxidative stress observed in osteoarthritic diarthrodial joints.[40] Furthermore, vitamins B1 (thiamin), B3, B6, and E are associated with the formation of osteophytes which are characteristic of OA.[42] Vitamins B and C potentially play a role in protecting against OA as they have been shown to decrease knee pain in OA patients through anti-inflammatory pathways.[43] Fold change analysis showed that putative anti-inflammatory metabolites were downregulated in cartilage exposed to SM which could be indicative of the perturbations in cellular use of vitamins in anti-inflammatory pathways. A notable finding was the identification of SM-induced changes in metabolites secreted from cartilage explants into surrounding media that mapped to vitamin E and lysine metabolism. We have previously detected these pathways in human synovial fluid from osteoarthritic donors,[40] suggesting that even short-term SM exposure may induce metabolic shifts similar to that of early osteoarthritis and be detectable by sampling synovial fluid.

Other pathways responsible for the alteration of chondrocyte metabolism in response to SM include the carnitine shuttle, fatty acid metabolism, cholesterol and squalene biosynthesis, C21-steroid hormone metabolism, and linoleate, glycerophospholipid, acetyltransferase, and glycosphingolipid metabolism. Changes in lipid metabolism may be indicative of higher energy demands as a result of abnormal ECM remodeling and modifications of chondrocyte state.[44] The carnitine shuttle assists in the transport of long-chain fatty acids into the mitochondrial matrix for β-oxidation and energy production. Studies have shown that OA patients have lower levels of fatty acids in both serum and synovial fluid compared to healthy individuals.[45,46] Disruptions in fatty acid metabolism could account for the increased energy demand as a result of ECM remodeling. Obesity has been identified as a significant risk factor for the onset and progression of OA.[47] As such, the comorbidity of obesity and OA may be responsible for changes in cholesterol and squalene biosynthesis. C21-steroid hormones are derived from cholesterol and, therefore, are implicated in the pathogenesis of OA by default. Linoleate is a fatty acid that possesses anti-inflammatory properties and has been shown to ameliorate arthritic symptoms.[48,49] Simulated microgravity also induced changes in glycerophospholipid metabolism, which may be suggestive of changes in chondrocyte differentiation. A key class of enzymes in the de novo synthesis of glycerophospholipids, lysophosphatidyl acyltransferases, have been shown to play a role in the transition of chondrocytes to hypertrophic chondrocytes. Decreased expression of glycosphingolipids have previously been linked to OA.[50] The depletion of glycosphingolipids in chondrocytes enhances the development of OA by disrupting the organization of cartilage.

Interestingly, biopterin metabolism was downregulated in cartilage explants at the 1-day time point, and starch and sucrose metabolism was identified as a perturbed pathway in explants exposed to SM at the 4-day time point. Biopterin functions as a cofactor and assists in tryptophan metabolism, nitric oxide signaling, and synthesis of hormones and neurotransmitters. The molecule has previously been linked to OA, although its role in the onset of joint disease is not fully elucidated.[51] Disturbances in starch and sucrose metabolism have been indirectly linked to OA due to the increase in lactate levels as a result of joint inflammatory processes.[52] Importantly, there are few studies that investigate the roles of these molecules in the pathogenesis of OA. Therefore, the link between these molecules and the onset of joint disease currently remains relatively unclear and warrants further investigation.

Limitations

Although this study has identified significant metabolic changes that occur in chondrocytes as a result of exposure to microgravity, some notable limitations are worth addressing. First, this study is limited by small sample sizes. Future studies will need to possess greater sample sizes in order to confirm microgravity-induced metabolic changes detected in cartilage explants and their surrounding media. Second, this study obtained cartilage explants from a single male donor who had no evidence of joint disease. Thus, this study is limited by potential confounding variables. Future work will take into consideration sex-related and age-related differences by studying SM-induced metabolic changes in cartilage explants from a variety of donors.[53] Third, this study solely used global metabolomics to map metabolite features to their potential identities and pathways. Follow-up studies will use targeted metabolomics to confirm the results indicated by this study.

Significance

When astronauts ascend into space, they are exposed to a reduced mechanical loading environment for prolonged periods of time. During this period, the astronauts' joints are not subjected to the forces that they would typically endure due to gravity and ambulation. This has been shown to be problematic by stimulating cartilage degradation and proteoglycan decomposition. The deterioration of major components of cartilage, including its matrix, can cause permanent and prolonged health effects for astronauts when they return from space due to the inability of cartilage to regenerate efficiently. Therefore, it is imperative that scientists at the National Aeronautics and Space Administration (NASA) understand the effects of a microgravity environment on cartilage in order to promote joint health and avoid long-term adverse effects of spaceflight on astronauts' joints. The results herein showcase a novel method for studying chondrocyte mechanotransduction in a manner that more accurately reflects chondrocyte behavior *in vivo*. To our knowledge, this study is the first to map global metabolic changes in cartilage in response to short-term simulated microgravity exposure to gain insight into the risk of developing osteoarthritis post-spaceflight.

References

(1) Sophia Fox, A. J., Bedi, A., & Rodeo, S. A. (2009). The basic science of articular cartilage: structure, composition, and function. *Sports health*, *1*(6), 461–468. https://doi.org/10.1177/1941738109350438

(2) Lahm, A., Mrosek, E., Spank, H., Erggelet, C., Kasch, R., Esser, J., & Merk, H. (2010). Changes in content and synthesis of collagen types and proteoglycans in osteoarthritis of the knee joint and comparison of quantitative analysis with Photoshop-based image analysis. Archives of orthopaedic and trauma surgery, 130(4), 557–564. https://doi.org/10.1007/s00402-009-0981-y

(3) Comfort, P., McMahon, J. J., Jones, P. A., Cuthbert, M., Kendall, K., Lake, J. P., & Haff, G. G. (2021). Effects of Spaceflight on Musculoskeletal Health: A Systematic Review and Meta-analysis, Considerations for Interplanetary Travel. *Sports medicine (Auckland, N.Z.)*, *51*(10), 2097–2114. https://doi.org/10.1007/s40279-021-01496-9

(4) Dreiner M, Willwacher S, Kramer A, Kümmel J, Frett T, Zaucke F, Liphardt A-M, Gruber M and Niehoff A (2020) Short-term Response of Serum Cartilage Oligomeric Matrix Protein to Different Types of Impact Loading Under Normal and Artificial Gravity. *Front. Physiol*. 11:1032. doi: 10.3389/fphys.2020.01032

(5) Ikenoue, T., Trindade, M. C., Lee, M. S., Lin, E. Y., Schurman, D. J., Goodman, S. B., & Smith, R. L. (2003). Mechanoregulation of human articular chondrocyte aggrecan and type II collagen expression by intermittent hydrostatic pressure in vitro. *Journal of orthopaedic research: official publication of the Orthopaedic Research Society*, *21*(1), 110–116. https://doi.org/10.1016/S0736-0266(02)00091-8

(6) Lee, D. A., & Bader, D. L. (1997). Compressive strains at physiological frequencies influence the metabolism of chondrocytes seeded in agarose. *Journal of orthopaedic research: official publication of the Orthopaedic Research Society*, *15*(2), 181–188. https://doi.org/10.1002/jor.1100150205

(7) Shelton, J. C., Bader, D. L., & Lee, D. A. (2003). Mechanical conditioning influences the metabolic response of cell-seeded constructs. *Cells, tissues, organs*, *175*(3), 140–150. https://doi.org/10.1159/000074630

(8) Manninen, P., Riihimaki, H., Heliovaara, M., & Suomalainen, O. (2001). Physical exercise and risk of severe knee osteoarthritis requiring arthroplasty. *Rheumatology (Oxford, England)*, *40*(4), 432–437. https://doi.org/10.1093/rheumatology/40.4.432

(9) Yokota, H., Leong, D. J., & Sun, H. B. (2011). Mechanical loading: bone remodeling and cartilage maintenance. *Current osteoporosis reports*, *9*(4), 237–242. https://doi.org/10.1007/s11914-011-0067-y

(10) Henao-Murillo, L., Pastrama, M. I., Ito, K., & van Donkelaar, C. C. (2021). The Relationship Between Proteoglycan Loss, Overloading-Induced Collagen Damage, and Cyclic Loading in Articular Cartilage. Cartilage, 13(2_suppl), 1501S–1512S. https://doi.org/10.1177/1947603519885005

(11) Nomura, M., Sakitani, N., Iwasawa, H., Kohara, Y., Takano, S., Wakimoto, Y., Kuroki, H., & Moriyama, H. (2017). Thinning of articular cartilage after joint unloading or immobilization. An experimental investigation of the pathogenesis in mice. *Osteoarthritis and cartilage*, *25*(5), 727–736. https://doi.org/10.1016/j.joca.2016.11.013

(12) Willey, J. S., Kwok, A. T., Moore, J. E., Payne, V., Lindburg, C. A., Balk, S. A., Olson, J., Black, P. J., Walb, M. C., Yammani, R. R., & Munley, M. T. (2016). Spaceflight-

Relevant Challenges of Radiation and/or Reduced Weight Bearing Cause Arthritic Responses in Knee Articular Cartilage. *Radiation research*, *186*(4), 333–344. https://doi.org/10.1667/RR14400.1

(13) Hudelmaier, M., Glaser, C., Hausschild, A., Burgkart, R., & Eckstein, F. (2006). Effects of joint unloading and reloading on human cartilage morphology and function, muscle cross-sectional areas, and bone density - a quantitative case report. *Journal of musculoskeletal & neuronal interactions*, *6*(3), 284–290.

(14) Ganse, B., Cucchiarini, M., & Madry, H. (2022). Joint Cartilage in Long-Duration Spaceflight. *Biomedicines*, *10*(6), 1356. https://doi.org/10.3390/biomedicines10061356

(15) Weitoft, T., Larsson, A., Saxne, T., & Rönnblom, L. (2005). Changes of cartilage and bone markers after intra-articular glucocorticoid treatment with and without postinjection rest in patients with rheumatoid arthritis. *Annals of the rheumatic diseases*, *64*(12), 1750–1753. https://doi.org/10.1136/ard.2004.035022

(16) Liphardt, A. M., Mündermann, A., Andriacchi, T. P., Achtzehn, S., Heer, M., & Mester, J. (2018). Sensitivity of serum concentration of cartilage biomarkers to 21-days of bed rest. *Journal of orthopaedic research: official publication of the Orthopaedic Research Society*, *36*(5), 1465–1471. https://doi.org/10.1002/jor.23786

(17) Hargens, A. R., & Vico, L. (2016). Long-duration bed rest as an analog to microgravity. *Journal of applied physiology (Bethesda, Md.: 1985)*, *120*(8), 891–903. https://doi.org/10.1152/japplphysiol.00935.2015

(18) Liphardt, A. M., Mündermann, A., Koo, S., Bäcker, N., Andriacchi, T. P., Zange, J., Mester, J., & Heer, M. (2009). Vibration training intervention to maintain cartilage thickness and serum concentrations of cartilage oligometric matrix protein (COMP) during immobilization. *Osteoarthritis and cartilage*, *17*(12), 1598–1603. https://doi.org/10.1016/j.joca.2009.07.007

(19) Hinterwimmer, S., Krammer, M., Krötz, M., Glaser, C., Baumgart, R., Reiser, M., & Eckstein, F. (2004). Cartilage atrophy in the knees of patients after seven weeks of partial load bearing. *Arthritis and rheumatism*, *50*(8), 2516–2520. https://doi.org/10.1002/art.20378

(20) Bader, D. L., Salter, D. M., & Chowdhury, T. T. (2011). Biomechanical influence of cartilage homeostasis in health and disease. *Arthritis*, *2011*, 979032. https://doi.org/10.1155/2011/979032

(21) Palmoski, M., Perricone, E., & Brandt, K. D. (1979). Development and reversal of a proteoglycan aggregation defect in normal canine knee cartilage after immobilization. *Arthritis and rheumatism*, *22*(5), 508–517. https://doi.org/10.1002/art.1780220511

(22) Ramkumar, P. N., Navarro, S. M., Becker, J., Ahmad, F., Minkara, A. A., Haeberle, H. S., Mont, M. A., & Williams, R. J. (2019). The Effects of Space Microgravity on Hip and Knee Cartilage: A New Frontier in Orthopaedics. *Surgical technology international*, *35*, 421–425.

(23) Bednarczyk E. (2022). Chondrocytes In Vitro Systems Allowing Study of OA. *International journal of molecular sciences*, *23*(18), 10308. https://doi.org/10.3390/ijms231810308

(24) Ulbrich, C., Westphal, K., Pietsch, J., Winkler, H. D., Leder, A., Bauer, J., Kossmehl, P., Grosse, J., Schoenberger, J., Infanger, M., Egli, M., & Grimm, D. (2010). Characterization of human chondrocytes exposed to simulated microgravity. *Cellular*

physiology and biochemistry: international journal of experimental cellular physiology, biochemistry, and pharmacology, *25*(4- 5), 551–560. https://doi.org/10.1159/000303059
(25) Mellor, L. F., Baker, T. L., Brown, R. J., Catlin, L. W., & Oxford, J. T. (2014). Optimal 3D culture of primary articular chondrocytes for use in the rotating wall vessel bioreactor. *Aviation, space, and environmental medicine*, *85*(8), 798–804. https://doi.org/10.3357/ASEM.3905.2014
(26) Jutila, A. A., Zignego, D. L., Schell, W. J., & June, R. K. (2015). Encapsulation of chondrocytes in high-stiffness agarose microenvironments for in vitro modeling of osteoarthritis mechanotransduction. *Annals of biomedical engineering*, *43*(5), 1132–1144. https://doi.org/10.1007/s10439-014-1183-5
(27) Zignego, D. L., Jutila, A. A., Gelbke, M. K., Gannon, D. M., & June, R. K. (2014). The mechanical microenvironment of high concentration agarose for applying deformation to primary chondrocytes. *Journal of biomechanics*, *47*(9), 2143–2148. https://doi.org/10.1016/j.jbiomech.2013.10.051
(28) Fredrikson, J. P., Brahmachary, P. P., Erdoğan, A. E., Archambault, Z. K., Wilking, J. N., June, R. K., & Chang, C. B. (2022). Metabolomic Profiling and Mechanotransduction of Single Chondrocytes Encapsulated in Alginate Microgels. *Cells*, *11*(5), 900. https://doi.org/10.3390/cells11050900
(29) Wang, X., June, R. K., & Pierce, D. M. (2021). A 3-D constitutive model for finite element analyses of agarose with a range of gel concentrations. *Journal of the mechanical behavior of biomedical materials*, *114*, 104150. https://doi.org/10.1016/j.jmbbm.2020.104150
(30) Bergstrom, A. (2022). Global Metabolomic Profiles and Viability of Encapsulated Chondrocytes Exposed to Short-Term Simulated Microgravity. *Carroll Scholars*, 1-23. https://scholars.carroll.edu/handle/20.500.12647/10610
(31) Wang, Q., Zheng, Y. P., Wang, X. Y., Huang, Y. P., Liu, M. Q., Wang, S. Z., Zhang, Z. K., & Guo, X. (2010). Ultrasound evaluation of site-specific effect of simulated microgravity on articular cartilage. *Ultrasound in medicine & biology*, *36*(7), 1089–1097. https://doi.org/10.1016/j.ultrasmedbio.2010.04.018
(32) Sibonga, J. D., Zhang, M., Evans, G. L., Westerlind, K. C., Cavolina, J. M., Morey-Holton, E., & Turner, R. T. (2000). Effects of spaceflight and simulated weightlessness on longitudinal bone growth. *Bone*, *27*(4), 535–540. https://doi.org/10.1016/s8756-3282(00)00352-5
(33) Kwok, A.T., Mohamed, N.S., Plate, J.F. *et al.* Spaceflight and hind limb unloading induces an arthritic phenotype in knee articular cartilage and menisci of rodents. *Sci Rep* **11**, 10469 (2021). https://doi.org/10.1038/s41598-021-90010-2
(34) Fitzgerald, J., Endicott, J., Hansen, U., & Janowitz, C. (2019). Articular cartilage and sternal fibrocartilage respond differently to extended microgravity. *NPJ microgravity*, *5*, 3. https://doi.org/10.1038/s41526-019-0063-6
(35) Ramachandran, V., Wang, R., Ramachandran, S. S., Ahmed, A. S., Phan, K., & Antonsen, E. L. (2018). Effects of spaceflight on cartilage: implications on spinal physiology. *Journal of spine surgery (Hong Kong)*, *4*(2), 433–445. https://doi.org/10.21037/jss.2018.04.07
(36) Takebe, T., Kobayashi, S., Kan, H., Suzuki, H., Yabuki, Y., Mizuno, M., Adegawa, T., Yoshioka, T., Tanaka, J., Maegawa, J., & Taniguchi, H. (2012). Human elastic cartilage engineering from cartilage progenitor cells using rotating wall vessel bioreactor.

Transplantation proceedings, *44*(4), 1158–1161. https://doi.org/10.1016/j.transproceed.2012.03.038

(37) Carlson, A. K., Rawle, R. A., Adams, E., Greenwood, M. C., Bothner, B., & June, R. K. (2018). Application of global metabolomic profiling of synovial fluid for osteoarthritis biomarkers. *Biochemical and biophysical research communications*, *499*(2), 182–188. https://doi.org/10.1016/j.bbrc.2018.03.117

(38) Zhai G. (2019). Alteration of Metabolic Pathways in Osteoarthritis. *Metabolites*, *9*(1), 11. https://doi.org/10.3390/metabo9010011

(39) Van Pevenage, P. M., Birchmier, J. T., & June, R. K. (2023). Utilizing metabolomics to identify potential biomarkers and perturbed metabolic pathways in osteoarthritis: A systematic review. *Seminars in arthritis and rheumatism*, *59*, 152163. https://doi.org/10.1016/j.semarthrit.2023.152163

(40) Carlson, A. K., Rawle, R. A., Wallace, C. W., Brooks, E. G., Adams, E., Greenwood, M. C., Olmer, M., Lotz, M. K., Bothner, B., & June, R. K. (2019). Characterization of synovial fluid metabolomic phenotypes of cartilage morphological changes associated with osteoarthritis. *Osteoarthritis and cartilage*, *27*(8), 1174–1184. https://doi.org/10.1016/j.joca.2019.04.007

(41) Jay, G. D., & Waller, K. A. (2014). The biology of lubricin: near frictionless joint motion. *Matrix biology: journal of the International Society for Matrix Biology*, *39*, 17–24. https://doi.org/10.1016/j.matbio.2014.08.008

(42) Muraki, S., Akune, T., En-yo, Y., Yoshida, M., Tanaka, S., Kawaguchi, H., Nakamura, K., Oka, H., & Yoshimura, N. (2014). Association of dietary intake with joint space narrowing and osteophytosis at the knee in Japanese men and women: the ROAD study. *Modern rheumatology*, *24*(2), 236–242. https://doi.org/10.3109/14397595.2013.854055

(43) Dehghan M. (2015). Comparative effectiveness of B and e vitamins with diclofenac in reducing pain due to osteoarthritis of the knee. *Medical archives (Sarajevo, Bosnia and Herzegovina)*, *69*(2), 103–106. https://doi.org/10.5455/medarh.2015.69.103-106

(44) Zignego, D. L., Hilmer, J. K., & June, R. K. (2015). Mechanotransduction in primary human osteoarthritic chondrocytes is mediated by metabolism of energy, lipids, and amino acids. *Journal of biomechanics*, *48*(16), 4253–4261. https://doi.org/10.1016/j.jbiomech.2015.10.038

(45) Tootsi, K., Kals, J., Zilmer, M., Paapstel, K., Ottas, A., & Märtson, A. (2018). Medium- and long-chain acylcarnitines are associated with osteoarthritis severity and arterial stiffness in end-stage osteoarthritis patients: a case-control study. *International journal of rheumatic diseases*, *21*(6), 1211–1218. https://doi.org/10.1111/1756-185X.13251

(46) Zhang, W., Likhodii, S., Zhang, Y., Aref-Eshghi, E., Harper, P. E., Randell, E., Green, R., Martin, G., Furey, A., Sun, G., Rahman, P., & Zhai, G. (2014). Classification of osteoarthritis phenotypes by metabolomics analysis. *BMJ open*, *4*(11), e006286. https://doi.org/10.1136/bmjopen-2014-006286

(47) Bliddal, H., Leeds, A. R., & Christensen, R. (2014). Osteoarthritis, obesity and weight loss: evidence, hypotheses and horizons - a scoping review. *Obesity reviews: an official journal of the International Association for the Study of Obesity*, *15*(7), 578–586. https://doi.org/10.1111/obr.12173

(48) Geetha, T., & Varalakshmi, P. (1999). Effect of lupeol and lupeol linoleate on lysosomal enzymes and collagen in adjuvant-induced arthritis in rats. *Molecular and cellular biochemistry*, *201*(1-2), 83–87. https://doi.org/10.1023/a:1007056300503
(49) Geetha, T., & Varalakshmi, P. (2001). Anti-inflammatory activity of lupeol and lupeol linoleate in rats. *Journal of ethnopharmacology*, *76*(1), 77–80. https://doi.org/10.1016/s0378-8741(01)00175-1
(50) Seito, N., Yamashita, T., Tsukuda, Y., Matsui, Y., Urita, A., Onodera, T., Mizutani, T., Haga, H., Fujitani, N., Shinohara, Y., Minami, A., & Iwasaki, N. (2012). Interruption of glycosphingolipid synthesis enhances osteoarthritis development in mice. *Arthritis and rheumatism*, *64*(8), 2579–2588. https://doi.org/10.1002/art.34463
(51) Hagihara, M., Nagatsu, T., Ohhashi, M., & Miura, T. (1990). Concentrations of neopterin and biopterin in serum from patients with rheumatoid arthritis or systemic lupus erythematosus and in synovial fluid from patients with rheumatoid or osteoarthritis. *Clinical chemistry*, *36*(4), 705–706.
(52) Alarcon, P., Hidalgo, A. I., Manosalva, C., Cristi, R., Teuber, S., Hidalgo, M. A., & Burgos, R. A. (2019). Metabolic disturbances in synovial fluid are involved in the onset of synovitis in heifers with acute ruminal acidosis. *Scientific reports*, *9*(1), 5452. https://doi.org/10.1038/s41598-019-42007-1
(53) Welhaven, H. D., Welfley, A. H., Pershad, P., Satalich, J., O'Connell, R., Bothner, B., Vap, A. R., & June, R. K. (2023). Metabolomic Phenotypes Reflect Patient Sex and Injury Status: A Cross-Sectional Analysis of Human Synovial Fluid. *bioRxiv: the preprint server for biology*, 2023.02.03.527040. https://doi.org/10.1101/2023.02.03.527040